PROCEEDINGS OF SCIENCE

Charmed and strange pseudoscalar meson decay constants from HISQ simulations

A. Bazavov[a]*, C. Bernard[† b], C. Bouchard[c], C. DeTar[d], D. Du[e], A.X. El-Khadra[e,f], J. Foley[d], E.D. Freeland[g], E. Gámiz[h], Steven Gottlieb[i], U.M. Heller[j], J. Kim[k‡], J. Komijani[b], A.S. Kronfeld[f], J. Laiho[l§], L. Levkova[d], P.B. Mackenzie[f], E.T. Neil[f¶], J.N. Simone[f], R.L. Sugar[m], D. Toussaint[‖k], R.S. Van de Water[f], and R. Zhou[i]**

[a] *Department of Physics, Brookhaven National Laboratory,[††] Upton, NY 11973, USA*
[b] *Department of Physics, Washington University, St. Louis, MO 63130, USA*
[c] *Department of Physics, The Ohio State University, Columbus, OH 43210, USA*
[d] *Department of Physics and Astronomy, University of Utah, Salt Lake City, UT 84112, USA*
[e] *Physics Department, University of Illinois, Urbana, IL 61801, USA*
[f] *Fermi National Accelerator Laboratory,[‡‡] Batavia, IL 60510, USA*
[g] *Department of Physics, Benedictine University, Lisle, IL 60532, USA*
[h] *CAFPE and Departamento de Física Teórica y del Cosmos, Universidad de Granada, Granada, Spain*
[i] *Department of Physics, Indiana University, Bloomington, IN 47405, USA*
[j] *American Physical Society, One Research Road, Ridge, NY 11961, USA*
[k] *Physics Department, University of Arizona, Tucson, AZ 85721, USA*
[l] *SUPA, School of Physics and Astronomy, University of Glasgow, Glasgow G12 8QQ, UK*
[m] *Department of Physics, University of California, Santa Barbara, CA 93106, USA*

Fermilab Lattice and MILC Collaborations

E-mail: doug@physics.arizona.edu, cb@wustl.edu

We update our determinations of f_{D^+}, f_{D_s}, f_K, and quark mass ratios from simulations with four flavors of HISQ dynamical quarks. The availability of ensembles with light quarks near their physical mass means that we can extract physical results with only small corrections for valence- and sea-quark mass mistunings instead of a chiral extrapolation. The adjusted valence-quark masses and lattice spacings may be determined from an ensemble-by-ensemble analysis, and the results for the quark mass ratios then extrapolated to the continuum limit. Our central values of the charmed meson decay constants, however, come from an alternative analysis, which uses staggered chiral perturbation theory for the heavy-light mesons, and allows us to incorporate data at unphysical quark masses where statistical errors are often smaller. A jackknife analysis propagated through all of these steps takes account of the correlations among all the quantities used in the analysis. Systematic errors from the finite spatial size and EM effects are estimated by varying the parameters in the analysis, and systematic errors from the assumptions in the continuum extrapolation are estimated from the spread of values from different extrapolations.

31st International Symposium on Lattice Field Theory - LATTICE 2013
July 29 - August 3, 2013
Mainz, Germany

© Copyright owned by the author(s) under the terms of the Creative Commons Attribution-NonCommercial-ShareAlike Licence.

arXiv:1312.0149v1 [hep-lat] 30 Nov 2013

1. Introduction

The pseudoscalar meson decay constants f_K, f_{D^+} and f_{D_s}, together with experimental decay rate determinations, are the simplest, although not necessarily most precise, ways to determine V_{us}, V_{cd} and V_{cs}. These decay constants are obtained from the amplitude of a point-source and point-sink (or random wall equivalent) pseudoscalar correlator $A_{pt\text{-}pt}$

$$f_{pseudo} = (m_A + m_B)\sqrt{\frac{3VA_{pt\text{-}pt}}{2M^3_{pseudo}}} \quad , \tag{1.1}$$

where m_A and m_B are the quark masses, and V is the spatial volume.

Here we update our determinations of these decay constants, and the quark mass ratios that are also produced in the analysis, from our program of simulations using a one-loop Symanzik improved gauge action and the highly-improved staggered quark (HISQ) action [1]. The HISQ action reduces taste violation errors by roughly a factor of three compared with the asqtad action. Also, the charm quark dispersion relation is improved so that charm quarks can be treated with the same relativistic action as the light quarks. Our ensembles include four flavors of dynamical quarks. Although the effects of a sea charm quark are expected to be small, the cost of including them is very small.

2. Correlator masses and amplitudes

The first step in our analysis is to find the masses and amplitudes of the pseudoscalar meson correlators, M_{pseudo} and $A_{pt\text{-}pt}$ in Eq. (1.1). Our ensembles of lattices and many of their characteristics were presented in Ref. [2]. Table 1 shows the ensembles and numbers of lattices used in this analysis, while Table 2 shows the valence masses used in each ensemble. Our sources, and choices of fitting functions and fit ranges were presented in Ref. [3], so we simply present them without further discussion in Table 3.

3. Lattice spacing, quark masses and decay constants on each ensemble

After determining the amplitudes and masses for the pseudoscalar correlators for all of the valence-quark masses, we determine the lattice spacing and corrected quark masses on each ensemble. Figure 1 illustrates the first steps in this procedure. We begin by finding the valence mass

*Present address: Department of Physics and Astronomy, University of Iowa, Iowa City, IA 52245

†Speaker.

‡Present address: Lattice Gauge Theory Research Center, CTP, and FPRD, Department of Physics and Astronomy, Seoul National University, Seoul, 151-747, South Korea

§Present address: Department of Physics, Syracuse University, Syracuse, New York, USA

¶Present address: Department of Physics, University of Colorado, Boulder, CO 80309, USA and RIKEN-BNL Research Center, Brookhaven National Laboratory, Upton, NY 11973, USA

‖Speaker.

**Present address: Fermi National Accelerator Laboratory, Batavia, IL 60510, USA

††Operated by Brookhaven Science Associates, LLC, under Contract No. DE-AC02-98CH10886 with the U.S. Department of Energy.

‡‡Operated by Fermi Research Alliance, LLC, under Contract No. DE-AC02-07CH11359 with the U.S. Department of Energy.

Table 1: Primary lattice ensembles used in this calculation. These ensembles have m_s tuned close to its physical value. A $*$ in the N_{lats} column indicates that lattice generation is still in progress. m_π is in MeV. Ensembles with m_s less than its physical value are also included in the chiral fit in Sec. 4.

β	am_l	am_s	am_c	size	N_{lats}	a (fm)	L (fm)	$m_\pi L$	m_π
5.80	0.013	0.065	0.838	$16^3 \times 48$	1020	0.14985(38)	2.38	3.8	314
5.80	0.0064	0.064	0.828	$24^3 \times 48$	1000	0.15303(19)	3.67	4.0	214
5.80	0.00235	0.0647	0.831	$32^3 \times 48$	1000	0.15089(17)	4.83	3.2	130
6.00	0.0102	0.0509	0.635	$24^3 \times 64$	1040	0.12520(22)	3.00	4.5	299
6.00	0.00507	0.0507	0.628	$24^3 \times 64$	1020	0.12085(28)	2.89	3.2	221
6.00	0.00507	0.0507	0.628	$32^3 \times 64$	1000	0.12307(16)	3.93	4.3	216
6.00	0.00507	0.0507	0.628	$40^3 \times 64$	1028	0.12388(10)	4.95	5.4	214
6.00	0.00184	0.0507	0.628	$48^3 \times 64$	999	0.12121(10)	5.82	3.9	133
6.30	0.0074	0.037	0.440	$32^3 \times 96$	1011	0.09242(21)	2.95	4.5	301
6.30	0.00363	0.0363	0.430	$48^3 \times 96$	1000	0.09030(13)	4.33	4.7	215
6.30	0.0012	0.0363	0.432	$64^3 \times 96$	1031	0.08773(08)	5.62	3.7	130
6.72	0.0048	0.024	0.286	$48^3 \times 144$	1016	0.06132(22)	2.94	4.5	304
6.72	0.0024	0.024	0.286	$64^3 \times 144$	1166	0.05938(12)	3.79	4.3	224
6.72	0.0008	0.022	0.260	$96^3 \times 192$	583*	0.05678(06)	5.44	3.7	135

Table 2: Valence masses used on each ensemble. The sea-quark masses am_l, am_s and am_c are in lattice units, while the valence-quark masses are given as fractions of the sea strange or charm quark mass.

β	am_l	am_s	am_c	light masses m_A (m/m_s)	m_B (m/m_c)
5.80	0.013	0.065	0.838	0.1,0.15,0.2,0.3,0.4,0.6,0.8,1.0	0.9,1.0
5.80	0.0064	0.064	0.828	0.1,0.15,0.2,0.3,0.4,0.6,0.8,1.0	0.9,1.0
5.80	0.00235	0.0647	0.831	0.036,0.07,0.1,0.15,0.2,0.3,0.4,0.6,0.8,1.0	0.9,1.0
6.00	0.0102	0.0509	0.635	0.1,0.15,0.2,0.3,0.4,0.6,0.8,1.0	0.9,1.0
6.00	0.00507	0.0507	0.628	0.1,0.15,0.2,0.3,0.4,0.6,0.8,1.0	0.9,1.0
6.00	0.00507	0.0507	0.628	0.1,0.15,0.2,0.3,0.4,0.6,0.8,1.0	0.9,1.0
6.00	0.00507	0.0507	0.628	0.1,0.15,0.2,0.3,0.4,0.6,0.8,1.0	0.9,1.0
6.00	0.00507	0.0304	0.628	0.1,0.15,0.2,0.3,0.4,0.6,0.8,1.0	0.9,1.0
6.00	0.00507	0.00507	0.628	0.1,0.15,0.2,0.3,0.4,0.6,0.8,1.0	0.9,1.0
6.00	0.00184	0.0507	0.628	0.036,0.073,0.1,0.15,0.2,0.3,0.4,0.6,0.8,1.0	0.9,1.0
6.30	0.0074	0.037	0.440	0.1,0.15,0.2,0.3,0.4,0.6,0.8,1.0	0.9,1.0
6.30	0.00363	0.0363	0.430	0.1,0.15,0.2,0.3,0.4,0.6,0.8,1.0	0.9,1.0
6.30	0.0012	0.0363	0.432	0.033,0.066,0.1,0.15,0.2,0.3,0.4,0.6,0.8,1.0	0.9,1.0
6.72	0.0048	0.024	0.286	0.05,0.1,0.15,0.2,0.3,0.4,0.6,0.8,1.0	0.9,1.0
6.72	0.0024	0.024	0.286	0.05,0.1,0.15,0.2,0.3,0.4,0.6,0.8,1.0	0.9,1.0
6.72	0.0008	0.022	0.260	0.036,0.068,0.1,0.15,0.2,0.3,0.4,0.6,0.8,1.0	0.9,1.0

Table 3: Fit forms and minimum distance included for the two-point correlator fits. Here the fit form is the number of negative parity (*i.e.*, pseudoscalar) states "plus" the number of positive parity states. In cases when the valence quarks have equal masses, the opposite parity states are not present. In this work, the charm-charm fits are used only in computing the mass of the η_c meson, which serves as a check on the quality of our charm physics.

	light-light		light-charm		charm-charm	
	form	D_{min}	form	D_{min}	form	D_{min}
$a \approx 0.15$ fm	1+1	16	2+1	8	2+0	9
$a \approx 0.12$ fm	1+1	20	2+1	10	2+0	12
$a \approx 0.09$ fm	1+1	30	2+1	15	2+0	18
$a \approx 0.06$ fm	1+1	40	2+1	20	2+0	21
$a \approx 0.045$ fm	1+1	53	2+1	26	2+0	31

where M_π^2/f_π^2 has its physical value (adjusted for finite size effects), which is illustrated in the upper left panel of Fig. 1. Here the red horizontal line is the desired value, and the green vertical line, the resulting quark mass. In solving for this point, we use the NLO continuum chiral perturbation theory form for M_π/f_π and linear and quadratic analytic terms. Using $f_\pi = 130.41$ MeV, we fix the lattice spacing a. Then, interpolating in light quark mass to the value found above, we use "kaons" with strange valence mass at 1.0 and 0.8 times the sea strange quark mass. The quantity $2M_K^2 - M_\pi^2$ is linearly interpolated or extrapolated to the point where it reaches its physical value to determine the adjusted strange quark mass, as illustrated in the upper right panel of Fig. 1. Then (not illustrated in the figure), we perform a similar interpolation in M_{D_s} to determine the adjusted charm quark mass. Finally the difference of light quark masses $m_d - m_u$ is determined from the K_0–K^+ mass splitting after adjustments for electromagnetic effects [4]. The use of these masses to determine f_K, f_{D^+} and f_{D_s} is illustrated in the lower panel of Fig. 1. This shows the decay constants as a function of light quark mass, where the other quark mass has been interpolated or extrapolated to adjust the strange (lower points) or charm (upper points) mass determined above. We then interpolate in these points to light quark mass m_u, m_d or m_s to find f_K, f_{D^+} or f_{D_s} respectively.

4. Chiral perturbation theory analysis of f_{D^+} and f_{D_s}

The quark-mass and lattice-spacing dependence of the decay constant has been calculated at one loop in heavy-meson, rooted, all-staggered chiral perturbation theory (HMrASχPT) in Ref. [5]. At fixed heavy-quark mass m_Q, one may argue following Ref. [6] and using the power counting introduced by Boyd and Grinstein [7] that inclusion of hyperfine splittings (*e.g.*, $M_D^* - M_D$) and flavor splittings (*e.g.*, $M_{D_s} - M_D$), but no other $1/m_Q$ effects, constitutes a systematic approximation at NLO in HMrASχPT. With v denoting the light valence quark, X the v$\bar{\text{v}}$ valence meson, and

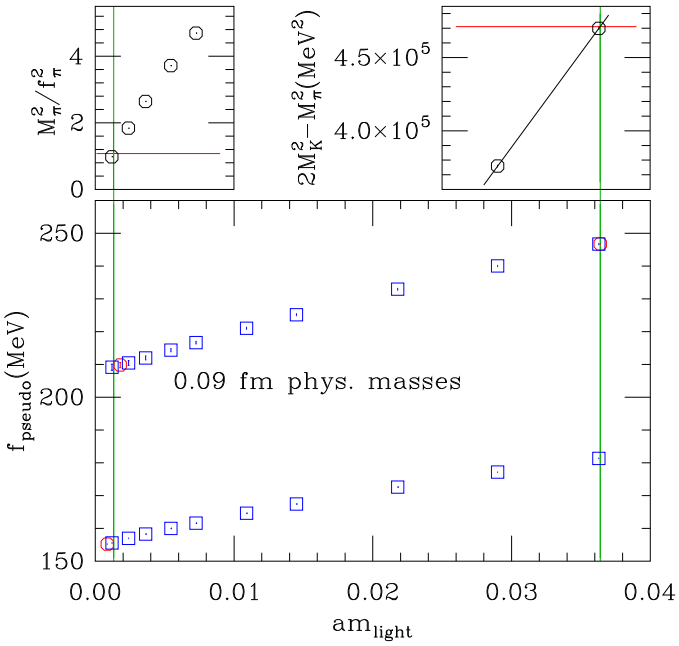


Figure 1: Illustration of the lattice spacing and quark mass tuning. The text contains a discussion of the procedure. This example is for the $a \approx 0.09$ fm ensemble with light quark mass near its physical value.

$\Phi_{D_\mathrm{v}} \equiv f_{D_\mathrm{v}}\sqrt{M_{D_\mathrm{v}}}$, Ref. [5] obtains for the pseudoscalar-taste heavy-light meson:

$$
\begin{aligned}
\Phi_{D_\mathrm{v}} = \Phi_0\Bigg\{ & 1 + \frac{1}{16\pi^2 f^2}\frac{1}{2}\Bigg(-\frac{1}{16}\sum_{\mathcal{S},\Xi}\ell(M^2_{\mathcal{S}\mathrm{v},\Xi}) - \frac{1}{3}\sum_{j\in\mathscr{M}_I^{(3,\mathrm{v})}}\frac{\partial}{\partial M^2_{X,I}}\left[R_j^{[3,3]}(\mathscr{M}_I^{(3,\mathrm{v})};\mu_I^{(3)})\ell(M_j^2)\right] \\
& - \Big(a^2\delta'_V \sum_{j\in\mathscr{M}_V^{(4,\mathrm{v})}}\frac{\partial}{\partial M^2_{X,V}}\left[R_j^{[4,3]}(\mathscr{M}_V^{(4,\mathrm{v})};\mu_V^{(3)})\ell(M_j^2)\right] + [V\to A]\Big) \\
& - 3g_\pi^2\frac{1}{16}\sum_{\mathcal{S},\Xi}J(M_{\mathcal{S}\mathrm{v},\Xi},\Delta^* + \delta_{\mathcal{S}\mathrm{v}}) - g_\pi^2\sum_{j\in\mathscr{M}_I^{(3,\mathrm{v})}}\frac{\partial}{\partial M^2_{X,I}}\left[R_j^{[3,3]}(\mathscr{M}_I^{(3,\mathrm{v})};\mu_I^{(3)})J(M_j,\Delta^*)\right] \\
& - 3g_\pi^2\Big(a^2\delta'_V\sum_{j\in\mathscr{M}_V^{(4,\mathrm{v})}}\frac{\partial}{\partial M^2_{X,V}}\left[R_j^{[4,3]}(\mathscr{M}_V^{(4,\mathrm{v})};\mu_V^{(3)})J(M_j,\Delta^*)\right] + [V\to A]\Big)\Bigg) \\
& + L_s(x_u + x_d + x_s) + L_\mathrm{v}x_\mathrm{v} + L_a\frac{x_{\bar{\Delta}}}{2}\Bigg\}\,,
\end{aligned}
\tag{4.1}
$$

where Φ_0, L_s, L_v, and L_a are low energy constants (LECs); the indices $\mathcal{S}$ and Ξ run over sea-quark flavors and meson tastes, respectively; Δ^* is the lowest-order hyperfine splitting; $\delta_{\mathcal{S}\mathrm{v}}$ is the flavor splitting between a heavy-light meson with light quark of flavor $\mathcal{S}$ and one of flavor v; and g_π is the D-D^*-π coupling. The chiral logarithm functions ℓ and J, and the residue functions $R_j^{[n,k]}$ and mass sets $\mathscr{M}^{(3,\mathrm{v})}$, $\mathscr{M}^{(4,\mathrm{v})}$, and $\mu^{(3)}$, are defined in Refs. [5, 8]. Subscripts on these mass sets indicate the

taste. We define dimensionless quark masses and a measure of the taste splitting by

$$x_{u,d,s,\mathrm{v}} \equiv \frac{4B}{16\pi^2 f_\pi^2} m_{u,d,s,\mathrm{v}} \,, \qquad\qquad x_{\bar{\Delta}} \equiv \frac{2}{16\pi^2 f_\pi^2} \bar{\Delta} \,, \tag{4.2}$$

where B is the LEC that gives the Goldstone pion mass $M_\pi^2 = B(m_u + m_d)$, and $\bar{\Delta}$ is the mean-squared pion taste splitting. The x_i are the natural variables of HMrASχPT; the LECs L_s, L_v, and L_a are therefore expected to be $\mathcal{O}(1)$. All ensembles in the current analysis have degenerate light quarks: $x_u = x_d \equiv x_l$. The taste splittings have been determined to $\sim$1–10% precision [2] and are used as input to Eq. (4.1), as are the taste-breaking hairpin parameters δ'_A and δ'_V, whose ranges are taken from chiral fits to light pseudoscalar mesons [9].

While Eq. (4.1) is a systematic NLO approximation for the decay constant at fixed m_Q, we have data on each ensemble with two different values of the (valence) charm mass: m_c and $0.9m_c$, where m_c is the value of the sea charm mass of the ensembles, and is itself not precisely equal to the physical charm mass m_c^{phys} because of tuning errors. In order to fit this data, we allow the LEC Φ_0 to depend on m_Q as suggested by HQET; for acceptable fits we need to introduce $1/m_Q$ and $1/m_Q^2$ terms. Furthermore, Φ_0 has generic lattice-spacing dependence that must be included to obtain good fits. With HISQ quarks, the leading generic discretization errors are $\mathcal{O}(\alpha_s a^2)$. But because the high degree of improvement in the HISQ action drastically reduces the coefficient of these leading errors, formally higher $\mathcal{O}(a^4)$ errors are also apparent. (See, for example, f_K/f_π *vs.* a^2 in Ref. [10].)

In Eq. (4.1), we thus replace

$$\Phi_0 \to \Phi_0 \left(1 + k_1 \frac{\Lambda_{\mathrm{QCD}}}{m_Q} + k_2 \frac{\Lambda_{\mathrm{QCD}}^2}{m_Q^2}\right) \left(1 + c_1 \alpha_s a^2 + c_2 a^4\right) , \tag{4.3}$$

where the k_i are new physical LECs, and c_i are additional fit parameters. In cases where the valence and sea values of the charm quark mass differ, m_Q in Eq. (4.3) is taken to denote the valence mass. Dependence on the charm sea mass over the $\sim$10% range of variation of m_Q is probably extremely small, since one expects that even the existence of a charm quark in the sea (*i.e.*, the difference between 2+1+1 and 2+1 simulations) is a small ($\lesssim$1%) effect.

Generic dependence on a is also allowed for the physical LECs L_s, L_v, k_1 and k_2. However, because these parameters first appear at NLO in the chiral or HQET expansions, it is sufficient to include only the leading a-dependence, for example:

$$L_\mathrm{v} \to L_\mathrm{v} + L_{\mathrm{v}\delta} \alpha_s a^2 \tag{4.4}$$

Thus we add 4 fit parameters related to generic discretization effects: $L_{\mathrm{v}\delta}$, $L_{\mathrm{s}\delta}$, $k_{1\delta}$, and $k_{2\delta}$. There are also 3 parameters related to taste-violation effects: L_a, δ'_A and δ'_V. These parameters are taken proportional to the measured average taste splitting $\bar{\Delta}$, which depends on a approximately as $\alpha_s^2 a^2$ [2]. In addition, we find that m_Q-dependent discretization errors must be considered if data at the coarsest lattice spacing ($a \approx 0.15$ fm) is included in the fits. This is not surprising because $am_c^{\mathrm{phys}} \approx 0.85$ at this lattice spacing, which by the power counting estimates of Ref. [1] suggests $\sim$5% discretization errors (although this may be reduced somewhat by dimensionless factors). We therefore add $c_3 \alpha_s (am_Q)^2 + c_4 (am_Q)^4$ to the analytic terms in Eq. (4.1). If the $a \approx 0.15$ fm data is omitted, good fits may be obtained with c_3 and c_4 set to zero.

For the LEC g_π, a reasonable range is $g_\pi = 0.53(8)$, which comes from recent lattice calculations [11, 12]. However, when this central value and range are included as Bayesian priors, fits to our full data set tend to pull g_π low, several sigma below 0.53. Hence, we simply fix $g_\pi = 0.45$, 1-sigma below its nominal value, in our current central fits. This problem is ameliorated for alternative fits, used to estimate the systematic errors, that drop the data at $a \approx 0.15$ fm. Other alternatives considered are to allow g_π to be a free parameter, or to keep it fixed at its nominal value.

Because we have precise data ($\sim$0.2% statistical errors) and 314 to 366 data points (depending on whether $a \approx 0.15$ fm is included), NLO HMrASχPT is not adequate to describe the quark mass dependence, in particular for masses near m_s. We therefore include all NNLO and NNNLO mass-dependent analytic terms. There are 4 independent functions of x_v, x_l and x_s at NNLO and 7 at NNNLO, for a total of 11 additional parameters. Our central fit then has 28 fit parameters, while alternative fits have between 27 and 31 parameters.

Relative scale setting is done using f_{p4s} [2], which is the light-light pseudoscalar decay constant at a fiducial point with both valence masses equal to $m_{p4s} \equiv 0.4 m_s^{\rm phys}$, and with the sea-quark masses physical. It is determined in lattice units on the physical-mass ensembles, with small adjustments for mistunings using nearby ensembles. We use a mass-independent scale-setting scheme: by definition, all ensembles at the same β have the same scale as the physical-mass ensemble. The ratio f_{p4s}/M_{p4s}, where M_{p4s} is the meson mass at the fiducial point, is used to (re-)tune m_s to its physical value. Values of the ratio and of f_{p4s} in physical units come from the analysis on the physical ensembles only, as described above. That analysis also gives the needed quark mass ratios m_c/m_s, m_s/m_l and m_u/m_d.

Figure 2 shows our central fit to partially quenched data at all four lattice spacings. The fit includes additional data (not shown) from ensembles at $a \approx 0.12$ fm ($\beta = 6.0$) with m_s lighter than physical or with volumes $24^3 \times 64$ and $40^3 \times 64$ (see Table 1), which were generated to check finite volume effects. We then extrapolate the parameters to the continuum, adjust the strange sea-quark mass and charm valence- and sea-quark masses to their physical values, and set the light sea-quark mass equal to the light valence mass (up to the small difference between m_d and $m_l = (m_u + m_d)/2$) giving the orange band. Putting in the physical light quark mass then gives the black burst, which is the result for Φ_{D^+}. Note that the effect of isospin violation in the valence quarks is included in our result; isospin violation in the sea is not included but is negligible. The biggest source of variation in the data in these four plots is not discretization errors, but mistunings of the strange and, most importantly, charm quark mass.

The statistical error in Φ_{D^+} and Φ_{D_s} given by the fit in Fig. 2 is only part of the total statistical error, since it does not include the statistical errors in the inputs of quark masses and lattice scale. To determine the total statistical error of each output quantity, we divide the full data set into 100 jackknife subensembles. The complete calculation, including the determination of the inputs, is performed on each subensemble, and the error is computed as usual from the variations over the subensembles. Each subensemble drops approximately 10 consecutive stored configurations (50 to 60 trajectories) from each (completed) ensemble. This procedure controls for autocorrelations, since all our measures of the autocorrelations of these quantities indicate that they are negligible after 4 or 8 consecutive configurations. For the incomplete physical-mass 0.06 fm ensemble with 583 configurations, we are forced to drop only about 6 consecutive stored configurations at a time. Our expectation is that the effect of any remaining autocorrelations, while perhaps not completely neg-

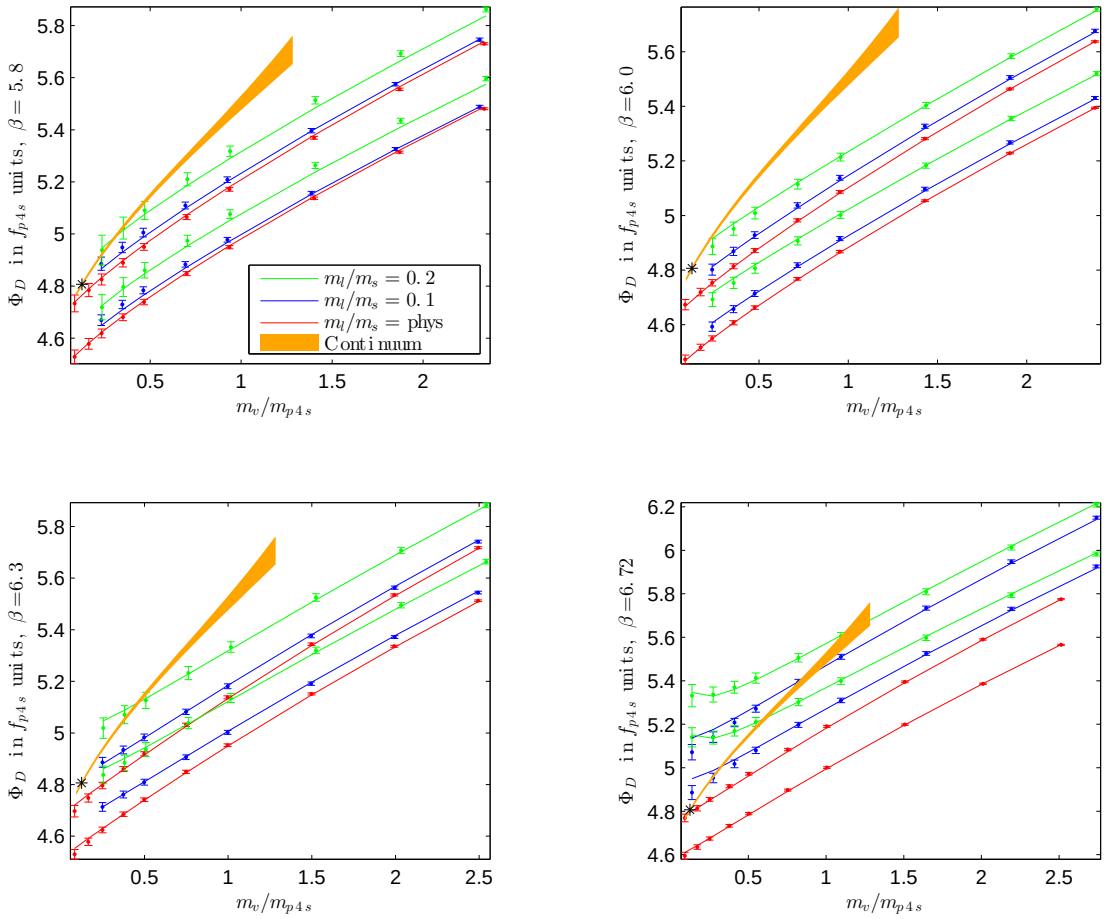


Figure 2: Simultaneous chiral fit to Φ_D as a function of m_v, the valence-quark mass (in units of m_{p4s}), at all four lattice spacings: $a \approx 0.15$ fm and 0.12 fm (top row), and 0.09 fm and 0.06 fm (bottom row). The colors denote different light sea-quark masses, as indicated. For each color there are two lines, one for heavy valence-quark mass $\approx m_c$ (higher line), and one for $\approx 0.9 m_c$. This fit has $\chi^2/\mathrm{dof} = 343.5/338$, giving $p = 0.41$. The orange band (which is identical in each plot, although the vertical and horizontal scales differ) gives the result after extrapolation to the continuum and adjustment of the strange and charm masses to their physical values. The width of the band shows the statistical error coming from the fit. The black bursts indicate the value of Φ_{D^+} at the physical light-quark mass point.

ligible, is small compared to other sources of error. The total statistical errors computed from the jackknife procedure are only about 10% larger than the statistical error from the chiral/continuum fit, indicating that the inputs are are statistically quite well determined.

Figure 3 illustrates how data for Φ_{D^+} and Φ_{D_s} depend on lattice spacing after adjustment to physical values of the quark masses (blue points). There is a 2–3% variation between these points and the continuum value (green point at $a^2 = 0$). Note that there is clear curvature in the plot, evidence of significant a^4 terms in addition to the formally leading $\alpha_s a^2$ terms. The red points show the contribution from the chiral logarithms (with known taste splittings) to the a^2 dependence of the chiral fit function. The green points show the corresponding contribution from the analytic fit parameters. The two effects are of comparable magnitudes but the relative sign changes with

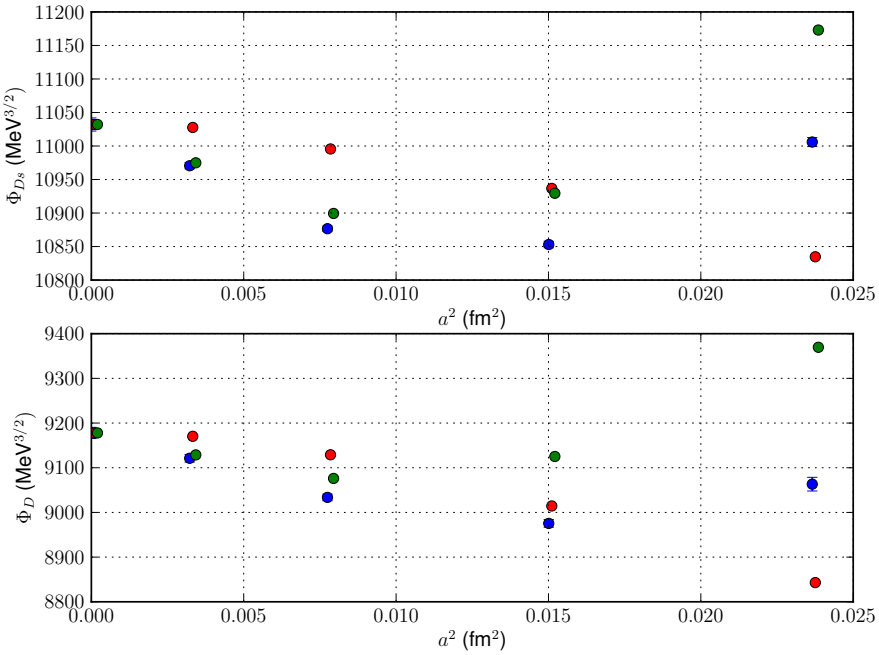


Figure 3: Lattice spacing dependence of Φ_{D^+} and Φ_{D_s}. The blue points show the lattice data, after adjustment for mistunings of valence-and sea-quark masses. The red points show the contribution from the chiral logarithms, while the green points show the a^2 dependence induced by the fit parameters. Red and green points overlap at $a = 0$ (only the green is visible).

lattice spacing; both are needed to describe the a^2 dependence of the data.

5. Continuum extrapolation and systematic errors

Our treatment of finite volume effects in the light quark meson masses and decay constants is described in Ref. [13]. To summarize, using NLO staggered chiral perturbation theory and results from three ensembles differing only in spatial size, we found the values that f_π, M_π, f_K and M_K would take in a 5.5 fermi box, the size of our physical quark mass ensembles. These adjusted values were then used in the tuning procedure described above. Afterwards, when f_K is reported, we reverse this correction to get the value at infinite volume. We use the difference between NLO staggered chiral perturbation theory and NNLO continuum chiral perturbation theory as an estimate of the remaining finite volume errors in the tuning procedure.

Electromagnetic effects in the kaon masses used in the tuning procedure were treated by using kaon masses adjusted for EM effects in the tuning procedure [4]. Remaining errors from these EM effects were estimated by varying the parameter that characterizes violation of Dashen's theorem, Δ_{EM}, by one standard deviation and by varying the less well understood shift in the average squared kaon mass by one half of its estimated value of 900 MeV^2. (The latter estimate does not include the effects of EM quark mass renormalization, which is not determined in the calculation of Ref. [4].)

For most quantities, our largest systematic error is the error from the continuum extrapolation and quark mass adjustments. In the tuning procedure which finds the valence-quark masses, and in the determination of f_K/f_π, this was done by trying several different fits, as illustrated in Fig. 4 for

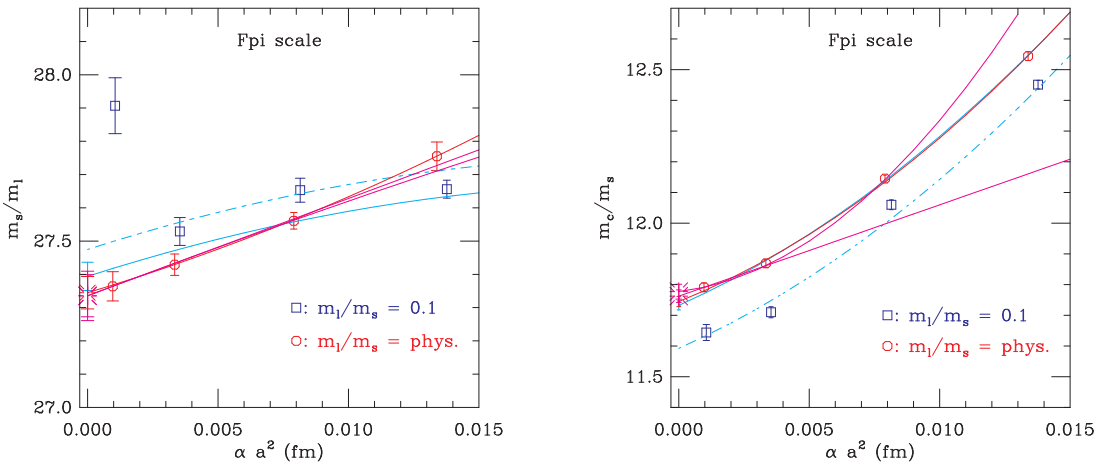


Figure 4: Quark mass ratios m_s/m_l and m_c/m_s on the physical and $0.1\,m_s$ ensembles, together with fits and continuum extrapolations described in the text. The red line is our preferred fit, which is quadratic in $a^2\alpha_{TV}$, determined from taste violations in the pion masses, using the physical quark mass ensembles with small corrections for valence quark mass mis-tuning. The cyan lines are a fit quadratic in $a^2\alpha_{TV}$ and linear in light valence mass, including the $0.1\,m_s$ ensembles. There the solid line is the fit evaluated at the physical light quark mass and the dashed line is the fit evaluated at $0.1\,m_s$. The magenta lines are zero degree-of-freedom fits to the physical ensembles, using a quadratic through the lowest three points or a line through the lowest two. Other fits not shown here are quadratic in $a^2\alpha_V$ or a^2.

m_s/m_l and m_c/m_s. Our first fit was quadratic in $\alpha_{TV}a^2$, where α_{TV} is proportional to a coupling constant determined from mass splittings among the different pion tastes, and linear in sea-quark m_l/m_s, using the physical quark mass and $m_l/m_s = 1/10$ ensembles. Central values for these quantities come from a fit that is quadratic in $\alpha_{TV}a^2$, using the physical quark mass ensembles with small adjustments (using the coefficient of m_l/m_s from the first fit) for sea-quark mass mistuning. We also considered fits to the physical mass ensembles that were quadratic in $\alpha_V a^2$ or a^2, where α_V is determined from the plaquette. Finally, we considered quadratic and linear extrapolations of the physical quark mass ensembles using the finest three and two lattice spacings respectively. We used the full range of variation among these extrapolations as the continuum extrapolation systematic error on the quark mass ratios and on f_K/f_π.

To determine the systematic error associated with the continuum extrapolation (and chiral interpolation) of the charmed decay constants in the chiral perturbation theory analysis, we rerun the analysis with alternative continuum/chiral fits, and with alternative inputs that come from different continuum extrapolations of the physical-mass analysis. We have a total of 15 acceptable ($p \geq 0.05$) versions of the continuum/chiral fits, which keep or drop the $a \approx 0.15$ fm ensemble, keep or drop $\alpha_s(am_c)^2$ and $(am_c)^4$ terms, constrain higher order chiral terms and/or discretization terms with priors or leave them unconstrained, add or omit additional parameters that permit the taste-violating parameters L_a, δ'_A and δ'_V to vary differently with lattice spacing than simply as $\bar{\Delta}$, *etc.* We also have the six versions of the continuum extrapolations used in the tuning procedure that leads to the inputs of quark mass and lattice scale. This gives a total of 90 versions of the analysis. Histograms of the 90 results for Φ_{D^+} and Φ_{D_s} are shown in Fig. 5. Conservatively, we

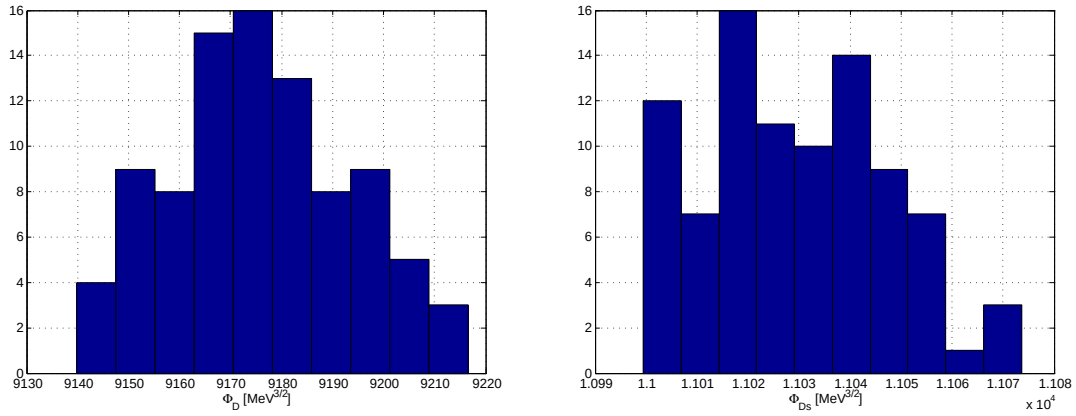


Figure 5: Histograms of Φ_{D^+} and Φ_{D_s} values obtained from various versions of the continuum/chiral extrapolation and various inputs of quark masses and scale values from the physical-mass analysis. Our central fit gives $\Phi_{D^+} = 9178$ MeV$^{3/2}$ and $\Phi_{D_s} = 11032$ MeV$^{3/2}$.

take the maximum difference seen in these results with our central values as the "self-contained" estimate of the continuum extrapolation errors within this chiral analysis. We now have carried out additional fits, beyond those shown at the conference, resulting in small increases in our estimated errors on some of the quantities. We now also choose a central fit that gives results close to the centers of the histograms, which results in more symmetrical error bars.

In practice, the NLO finite volume corrections are included in our fit function, Eq. (4.1), when it is applied to the data, and the volume is sent to infinity when the continuum results are extracted. We may conservatively estimate the residual finite volume error in the heavy-light data either by turning off all finite volume corrections and repeating the fit, or by using the current fit to find the size of the NLO finite volume correction on our most-important, 0.06 fm physical-mass ensemble. Yet another way to make the estimate is by direct comparison of our results on the $32^3 \times 64$, $\beta = 6.0$, $m_l = 0.1 m_s$ ensemble (which is similar in physical size to our other $m_l = 0.1 m_s$ ensembles) and the $40^3 \times 64$, $\beta = 6.0$, $m_l = 0.1 m_s$ ensemble. All three methods indicate that there are negligible direct finite volume effects in the heavy-light lattice data. Nevertheless, there are non-negligible finite volume effects in our final answers, which appear due to the scale setting in the light-quark sector through, ultimately, f_π. (The value of f_{p4s} in physical units that we use comes by comparison with f_π.) We then propagate the errors in the inputs through our analysis. Electromagnetic errors in the light quark masses are similarly propagated through our analysis.

6. Results

The results for D-meson decay constants from the self-contained chiral fit analysis are:

$$f_{D^+} = 212.3 \pm 0.3_{\rm stat} \pm 0.9_{a^2\,\rm extrap} \pm 0.3_{\rm FV} \pm 0.0_{\rm EM} \pm 0.3_{f_\pi\,\rm expt}\ \text{MeV} \quad (6.1)$$

$$f_{D_s} = 248.7 \pm 0.2_{\rm stat}\ {}^{+0.9}_{-0.7}|_{a^2\,\rm extrap} \pm 0.2_{\rm FV} \pm 0.1_{\rm EM} \pm 0.4_{f_\pi\,\rm expt}\ \text{MeV} \quad (6.2)$$

$$f_{D_s}/f_{D^+} = 1.1714(10)_{\rm stat}({}^{+23}_{-21})_{a^2\,\rm extrap}(3)_{\rm FV}(5)_{\rm EM} \quad (6.3)$$

It should be emphasized that the EM errors we estimate here, which come from effects on light-meson, and hence light-quark, masses, do not include the EM effects on the D_s mass, which we use

to fix the c-quark mass. We make a rough estimate of this omitted EM effect below. In addition, we note that we are computing the values the decay constants as they are conventionally defined, in a pure-QCD world. Comparison to experiment thus requires a matching of the decay rates between QCD and QCD+QED. The errors in such a matching are not included in our error estimates.

We take the central values and statistical errors in Eqs. (6.1) through (6.3) as our best estimates. For the continuum extrapolation error, we also consider the differences of the central values with corresponding quantities obtained by various continuum extrapolations of the straightforward analysis on the physical-mass ensembles, and take those differences as the error whenever they are larger than the self-contained error. The analysis on the physical-mass ensembles also gives alternative error estimates for the finite volume and EM errors, which however turn out to be the same as, or slightly smaller than, those in Eqs. (6.1) through (6.3). This procedure gives our current best (but still preliminary) results for f_{D^+}, f_{D_s} and f_{D_s}/f_{D^+}. We also include results for quark-mass ratios coming from the tuning procedure described in Sec. 3, and f_{K^+}/f_π coming from the ensemble-by-ensemble analysis:

$$m_c/m_s = 11.741(19)_{\rm stat}(59)_{\rm sys} \tag{6.4}$$

$$m_s/m_l = 27.366(52)_{\rm stat}(107)_{\rm sys} \tag{6.5}$$

$$m_u/m_d = 0.4619(48)_{\rm stat}(169)_{\rm sys} \tag{6.6}$$

$$f_{K^+}/f_\pi = 1.1957(10)_{\rm stat} \pm (25)_{\rm sys} \tag{6.7}$$

$$f_{D^+} = 212.3 \pm 0.3_{\rm stat}\, {}^{+0.9}_{-1.1}|_{a^2\,\rm extrap} \pm 0.3_{\rm FV} \pm 0.0_{\rm EM} \pm 0.3_{f_\pi\,\rm expt}\ \text{MeV} \tag{6.8}$$

$$f_{D_s} = 248.7 \pm 0.2_{\rm stat}\, {}^{+0.9}_{-1.4}|_{a^2\,\rm extrap} \pm 0.2_{\rm FV} \pm 0.1_{\rm EM} \pm 0.4_{f_\pi\,\rm expt}\ \text{MeV} \tag{6.9}$$

$$f_{D_s}/f_{D^+} = 1.1714(10)_{\rm stat}({}^{+29}_{-21})_{a^2\,\rm extrap}(3)_{\rm FV}(5)_{\rm EM} \tag{6.10}$$

The EM errors here do not include the effect of the EM contribution to the D_s mass, which has not been directly determined in QCD+QED simulations. This effect would change m_c/m_s and, in turn, f_{D^+} and f_{D_s}. We may roughly estimate the effect by assuming the EM effect on M_{D_s} is similar to that on m_K, namely a few MeV. This would change m_c/m_s by $\sim$0.01–0.03, f_{D^+} and f_{D_s} by $\sim$0.01–0.05 MeV, and f_{D_s}/f_{D^+} $\sim$0.0001–0.0003.

These decay constants have been computed by several groups using a variety of gauge and fermion actions. In Figs. 6 and 7 we compare the results in this work with previous computations of the decay constants.

Acknowledgments

This work was supported by the U.S. Department of Energy and National Science Foundation, by the URA Visiting Scholars' program (A.E-K.), and by the MINECO, Junta de Andalucía, and European Commission. Computation for this work was done at the Argonne Leadership Computing Facility (ALCF), the National Center for Atmospheric Research (UCAR), Bluewaters at the National Center for Supercomputing Resources (NCSA), the National Energy Resources Supercomputing Center (NERSC), the National Institute for Computational Sciences (NICS), the Texas Advanced Computing Center (TACC), and the USQCD facilities at Fermilab, under grants from the NSF and DOE.

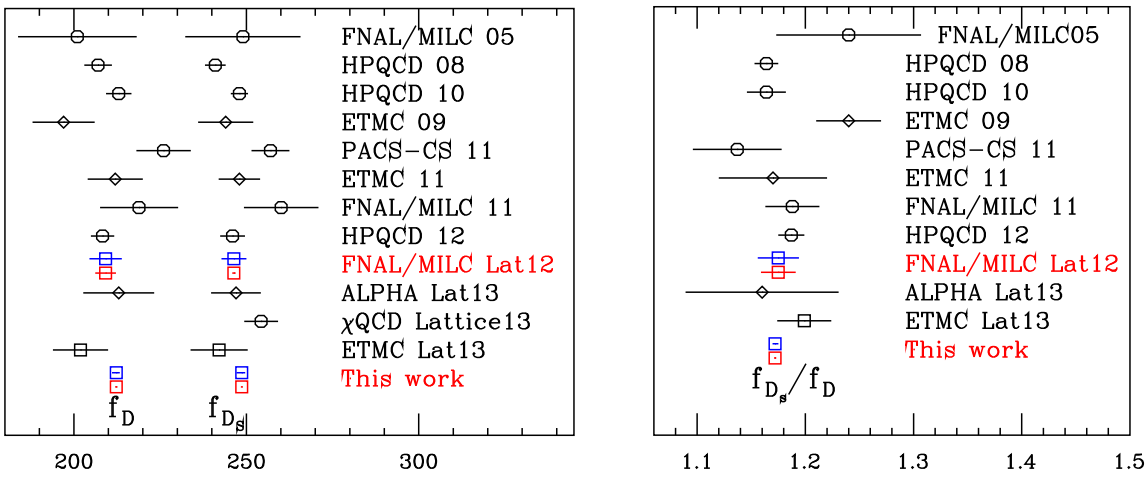


Figure 6: Lattice computations of f_D, f_{D_s} and f_{D_s}/f_D. Diamonds are $n_f = 2$ calculations, octagons $n_f = 2+1$ and squares $n_f = 2+1+1$. Earlier work is from references [14–24]. In the results from these proceedings and the FNAL/MILC Lattice 12 results, red points have statistical errors only, blue include systematic errors.

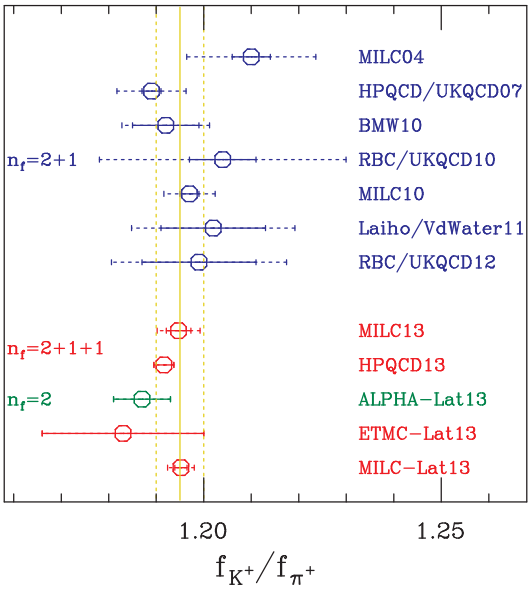


Figure 7: Determinations of f_K/f_π. Earlier work is from references [10, 24–31]. The vertical lines show the central value and errors of the FLAG 2+1+1 average [32].

References

[1] E. Follana *et al.* [HPQCD Collaboration], Phys. Rev. D **75**, (2007) 054502 [hep-lat/0610092].

[2] A. Bazavov *et al.* [MILC Collaboration], Phys. Rev. **D87**, 054505 (2013), [arXiv:1212.4768].

[3] A. Bazavov *et al.*, PoS(Lattice 2012)158, [arXiv:1212.0613].

[4] L. Levkova *et al.* [MILC Collaboration], PoS(Lattice2012)137; C. Bernard *et al.* [MILC Collaboration], PoS(CD12)030 [arXiv:1301.7137].

[5] J. Komijani and C. Bernard, PoS LAT2012 (2012) 199 [arXiv:1211.0785]; C. Bernard and J. Komijani, [arXiv:1309.4533].

[6] A. Bazavov *et al.* [Fermilab Lattice and MILC Collaborations], Phys. Rev. D **85**, 114506 (2012) [arXiv:1112.3051].

[7] C. G. Boyd and B. Grinstein, Nucl. Phys. **B442**, 205 (1995), [arXiv:hep-ph/9402340].

[8] C. Aubin and C. Bernard, Phys. Rev. D76, 014002 (2007), [arXiv:hep-lat/0704.0795].

[9] A. Bazavov *et al.* [MILC Collaboration], PoS LATTICE **2011**, 107 (2011) [arXiv:1111.4314 [hep-lat]], and work in progress.

[10] A. Bazavov *et al.* [MILC Collaboration], Phys. Rev. Lett. **110**, 172003 (2013).

[11] D. Becirevic and F. Sanfilippo, Phys. Lett. **B721**, 94 (2013) [arXiv:1210.5410]; K. U. Can, G. Erkol, M. Oka, A. Ozpineci, and T. T. Takahashi, Phys. Lett. **B719**, 103 (2013) [arXiv:1210.0869].

[12] W. Detmold, C. J. D. Lin, and S. Meinel, Phys. Rev. D**85**, 114508 (2012) [arXiv:1203.3378].

[13] A. Bazavov *et al.* [Fermilab Lattice and MILC Collaborations], PoS(Lattice 2012)159 [arXiv:1210.8431].

[14] C. Aubin *et al.* [Fermilab Lattice and MILC Collaborations], Phys. Rev. Lett. **95**, 122002(2005), [arXiv:hep-lat/0506030].

[15] E. Follana *et al.* [HPQCD Collaboration], Phys. Rev. Lett. **100**, 062002 (2008) [arXiv:0706.1726].

[16] C. Davies *et al.* [HPQCD Collaboration], Phys. Rev. D **82**, 114504 (2010) [arXiv:1008.4018].

[17] B. Blossier *et al.* [ETM Collaboration], JHEP **0907** 043 (2009) [arXiv:0904.0954].

[18] Y. Namekawa *et al.* [PACS-CS Collaboration], Phys. Rev. D **84** (2011) 074505 [arXiv:1104.4600].

[19] P. Dimopoulos *et al.* [ETM Collaboration], JHEP **01**, 046 (2012) [arXiv:1107.1441].

[20] J.A. Bailey *et al.* [Fermilab Lattice and MILC Collaborations], PoS(Lattice2011)320 [arXiv:1112.3978]; A. Bazavov *et al.* [Fermilab Lattice and MILC Collaborations], Phys. Rev. D **85** 114506 (2012), [arXiv:1112.3051].

[21] H. Na *et al.* [HPQCD Collaboration], Phys. Rev. D **85** 125029 (2012) [arXiv:1206.4936].

[22] Y. Yang, Y. Chien, Z. Liu, these proceedings

[23] J. Heitger, G. von Hippel, S. Schaefer and F. Virotta [ALPHA Collaboration], these proceedings.

[24] L. Riggio [ETM Collaboration], these proceedings.

[25] C. Aubin *et al.* [MILC Collaboration] Phys. Rev. **D** 70, 114501 (2004).

[26] E. Follana, C. T. H. Davies, G. P. Lepage and J. Shigemitsu [HPQCD/UKQCD Collaboration], Phys. Rev. Lett. **100** (2008) 062002 [arXiv:0706.1726].

[27] A. Bazavov *et al.* [MILC Collaboration], PoS LATTICE2010, 074 (2010).

[28] Y. Aoki *et al.* [RBC/UKQCD Collaboration], Phys. Rev. D**83** (2011) 074508 [arXiv:1011.0892].

[29] S. Dürr *et al.* [BMW Collaboration], Phys. Rev. D **81**, 054507 (2010) [arXiv:1001.4692].

[30] R.J. Dowdall, C.T.H. Davies, G.P. Lepage and C. McNeile [HPQCD Collaboration], [arXiv:1303.1670]; R. Dowdall *et al.*, these proceedings.

[31] S. Lottini [ALPHA Collaboration], these proceedings

[32] S. Aoki *et al.* [FLAG], arXiv:1310.8555 [hep-lat].